Precision & Performance Conference 2025, Cranfield University, UK, 17th- 20th November 2025

Finite Element Analysis of Mold Geometry Effects on Glass Flow and Stress in Wafer-Level Precision Glass Molding

Christian Strobl*[1], Anh Tuan Vu[1], Marcel Oppenberg[1], Thomas Hess[1], Cornelia Rojacher[1], Thomas Bergs[2]

[1]*Fraunhofer Institute for Production Technology*
[2]*RWTH Aachen University*

**Christian.strobl@ipt.fraunhofer.de*

Abstract
This study investigates the influence of inter-cavity geometry on the form filling behavior during isothermal Wafer-Level Glass Molding (WLGM) using numerical simulations based on the Finite Element Method (FEM). We analyze the flow of Schott B270® glass in a 5 x 5 lens array configuration, focusing on the effects of various geometric parameters such as bridge width, frustum height, and spacing between cavities. A Design of Experiments (DoE) approach, specifically Response Surface Methodology (RSM), is employed to optimize these parameters and assess their impact on glass flow and stress distribution.
The results indicate that a smaller initial contact area enhances the molding process by increasing local stresses, thereby facilitating glass flow into the cavities. The analysis of stress distribution reveals that shear stresses play a critical role in the forming process, as they promote more energy-efficient deformation compared to normal stresses. This is particularly beneficial due to the low compressibility of glass, which makes shear-induced deformation preferable over volumetric changes.
Notably, the study highlights the critical role of the pyramid angle and the distance between frustums in mitigating flow resistance and enhancing overall glass distribution. Our findings contribute valuable insights into the design of mold geometries for WLGM, enabling the production of high-precision optical components with reduced cycle times and improved material utilization.

Optics, Precision glass molding, Wafer level optics, Design of Experiments

1. Introduction

The demand for high-precision optics in large-volume markets is experiencing significant growth. Relevant application fields include consumer electronics, medical technology, semiconductors, projection systems, and lighting. Glass remains the material of choice due to its thermal stability, scratch resistance, and recyclability. Precision glass molding (PGM) enables the manufacturing of reproducible, high-quality optical components with form errors of peak to valley (P-V) < 1 µm [1]. However, a major drawback of this process is the long process cycle, which can extend up to 30 minutes per product unit.

Wafer-Level Glass Molding (WLGM) overcomes this limitation by enabling the simultaneous replication of multiple optics in a single molding step, followed by separation into individual components, thereby providing substantial scalability for mass production. In this method, a large-area glass wafer is pressed into a multi-cavity mold, allowing the parallel forming of several optical elements. Strobl *et al.* [2] and Vogel *et al.* [3] have highlighted the importance of WLGM in non-isothermal glass molding.

A central challenge in WLGM is the control of glass flow and stress evolution, which is crucial for achieving the desired form accuracy and surface quality of the molded optics. The large contact area between glass and mold wafers imposes mechanical constraints on the molding process due to its limited forming force capacity. Furthermore, interactions between adjacent cavities can lead to non-uniform flow behavior and inhomogeneous stress distributions within the glass wafer. Hünten *et al.* [4]and Liu *et al.* [5] proposed the use of frustum-shaped transition structures in isothermal WLGM to enhance the glass flow into the cavities. However, to date, the influence of the geometry parameters of these frustum structures on glass flow and stress formation has not been systematically investigated.

This paper presents a Finite Element Method (FEM)-based investigation to analyze the influence of mold-cavity geometry on glass flow and stress in WLGM. A Design of Experiments (DoE) approach is utilized to develop a Response Surface Methodology (RSM) that characterizes the design space. FEM simulations are performed to model various mold geometries, enabling a comprehensive quantitative and qualitative assessment of geometry-dependent glass flow and stress distributions within the molded wafer.

2. Methodology

The objective of this research is to investigate the influence of inter-cavity geometry on glass flow behavior and the resulting stress distribution during WLGM. A plano-convex spherical lens was selected as the demonstrator geometry for the individual optics. This choice enables a detailed analysis of the effects of inter-cavity design on glass flow.

Schott B270® glass was chosen due to its high transparency, excellent optical performance, and widespread use in precision optics manufacturing. Furthermore, its viscoelastic characteristics make it well-suited for glass molding [6-8].

2.1. Choice of influencing parameters

In this study, a 5 x 5 lens array in a square arrangement is examined. This configuration includes one central cavity (type 1), 16 outer cavities (type 3), and 8 intermediate cavities

(type 2) that are expected to be unaffected by either central or edge effects. Each cavity is designed as a spherical segment with a fixed radius r_L and maximum sag height h_L. All relevant geometric parameters of the mold are illustrated in Figure 1.

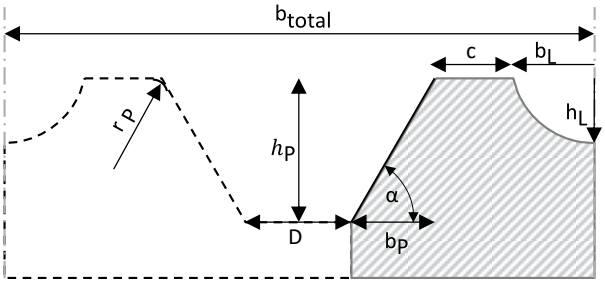

Figure 1. Geometric parameters considered in WLGM mold design.

The lens width (b_L) and lens height (h_L) are kept constant to evaluate the influence of the interstitial geometry on glass flow into the cavity, using a defined cavity geometry as a reference (eq. 1).

$$b_L = 2r_L \sin\left(\cos^{-1}\left(\frac{r_L - h_L}{r_L}\right)\right) \quad (1)$$

The frustum width (b_P) is directly dependent on the frustum height (h_P) and the pyramid angle (α), derived using trigonometric relations (eq. 2). To minimize factor interdependencies, b_P is not considered as an independent variable.

$$b_P = \frac{h_P}{\tan\alpha} \quad (2)$$

The lens spacing (b_{total}) is a critical factor for process scalability, defining the number of lenses producible per wafer area. It can be expressed as the sum of the lens width, frustum spacing, frustum width, and bridge width, including the adjacent radii (eq. 3). Due to its geometric dependence on other factors, b_{total} is not be analyzed separately from a process perspective.

$$b_{total} = D + b_L + 2\left(c + \frac{h_P}{\tan\alpha} + r_P \sin\alpha\right) \quad (3)$$

Instead, the frustum spacing (D) is considered as an influencing factor on the forming behavior.

The bridge width (c) represents the initial contact area between the glass and the mold surface. It is expected to have a significant effect on the stress distribution during molding, as the local stresses are inversely proportional to the contact area. A smaller contact area results in higher localized stresses.

The frustum radius (r_P) also affects the contact area as forming progresses. Variations in r_P are, thus, expected to influence the local stress concentration in the glass during the molding process.

The frustum height (h_P) indirectly determines the frustum width in conjunction with the pyramid angle (α). Since h_P and α define the volume of the glass reservoir that does not flow into the cavities, they significantly influence both flow dynamics and stress evolution. According to Liu *et al.* [5] and Hünten *et al.* [4], this reservoir influences the stress developed in the glass and form accuracy. The pyramid angle further affects the shrinkage and release of the glass after forming. In addition, the frustum spacing (D) impacts the reservoir size and the distance between adjacent cavities.

The initial dimensions (width and depth) of the glass preform are adapted to the mold design, while the glass thickness is kept constant for all configurations.

In this analysis, the form filling (Δ) is defined analogously to the center thickness of optical lenses, as illustrated in Figure 2.

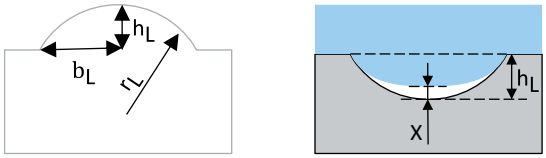

Figure 2. Design of the glass optics (left); relevant geometrical indicators for definition of form filling (right).

Here, x denotes the vertical distance between the lowest node of the glass and the mold cavity's centerpoint (eq. 4). The deviation from the target cavity height (h_L) serves as a measure of the filling ratio.

$$\Delta = \frac{h_L - x}{h_L} \quad (4)$$

2.2. Design of Experiments

The Design of Experiments (DoE) approach based on Response Surface Methodology (RSM) is performed using the five selected geometric factors indicated in table 1. The star points are centered within the feasible geometric domain to respect design limitations. By selecting the RSM, non-linear relationships among the chosen factors can be captured.

The experimental design consists of the full 2^k factorial design, representing all corner points of the factor space. Incorporating 2k star points extends the design to account for quadratic interactions, allowing for second-order response modeling. This design framework enables the assessment of linear, quadratic, and interaction effects among the influencing parameters.

Table 1. Definition of factors and factor ranges for the DoE.

Pyramid angle/°	Frustum radius/ 10^{-3} m	Bridge width/ 10^{-3} m	Frustum spacing/ 10^{-3} m	Frustum heigh/ 10^{-3} m
α	r_P	C	D	h_P
30 - 60	0.1 - 1	0.1 - 1	0 - 2	1 – 1.5

2.3. Finite Element Modeling

The Finite Element (FE) simulation of the isothermal WLGM was carried out using ABAQUS. The model represents a 2D cross-section of the mold–glass system and incorporates symmetry boundary conditions to reduce computational effort. To capture position-dependent effects across the wafer, three representative cavity locations were investigated: center (1), intermediate (2), and outer (3).

Stainless steel 1.4841 was chosen as the mold material, while Schott B270® served as the glass wafer. The wafer was molded at a forming temperature of 630 °C, corresponding to a viscosity of 9.5 dPas, demonstrating its suitable processing conditions for this glass type [6,7].

The viscoelastic behavior of the glass was modeled using a generalized Maxwell model. Coulomb friction was implemented with a coefficient of μ = 1.5 [9]. Preliminary experimental trials were carried out and confirmed that a forming pressure of 9.118 MPa ensures stable molding behavior of the glass wafer at the selected viscosity. To account for the varying cavity configurations, the applied force was linearly scaled with the corresponding mold area.

A constant pressing duration of 120 seconds was assumed for all simulations. Thermally coupled, linear plane-strain (CPE4T) were chosen as element type of the FE model.

3. Results

3.1. Influence of the inter-cavity geometry on the glass flow during WLGM

The analysis of the residual diagrams using Minitab software demonstrates that the prerequisites for conducting an analysis of variance (ANOVA) are satisfactorily met. Specifically, the independence of errors is ensured, the residuals follow a normal distribution, and the homogeneity of variances is confirmed.

Furthermore, the correlation among the three different cavities was examined using the Pearson correlation coefficient to quantify the degree of linear dependency. Notably, strong correlations were observed among all cavities, with the intermediate cavity exhibiting the highest correlation to both the center (1) and the outer (3) cavities, yielding values of 0.983 and 0.956, respectively. The Pareto diagrams (Figure 3) further confirm that all selected geometric factors exert a significant effect on the form filling behavior. These results validate the relevance of the frustum design and highlight the necessity for its geometric optimization.

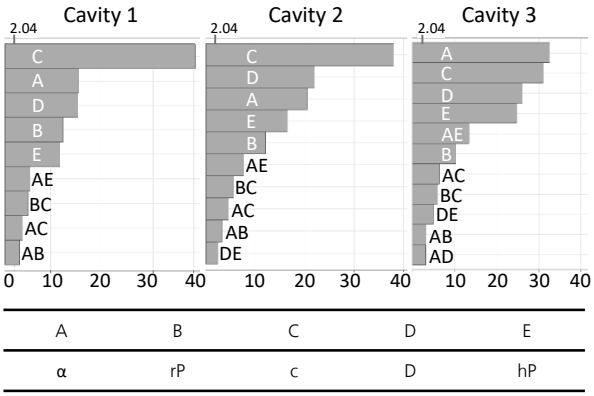

Figure 3. Pareto diagrams showing the relative significance of factors and their interactions

Although the correlations are high, the relative significance of parameters varies between cavities. In the cavity (1), the bridge width (c) emerges as the most significant factor. This trend also holds for the cavity (2), although the influence of the other parameters becomes more pronounced. In contrast, for the cavity (3), the angle (α) exhibits greater significance than the bridge width (c).

The main effect plots (Figure 4) reveal that optimal form filling across all cavities is achieved with a combination of a small bridge width, a small frustum radius, a flat pyramid angle, a high frustum height, and a large distance between the frustums.

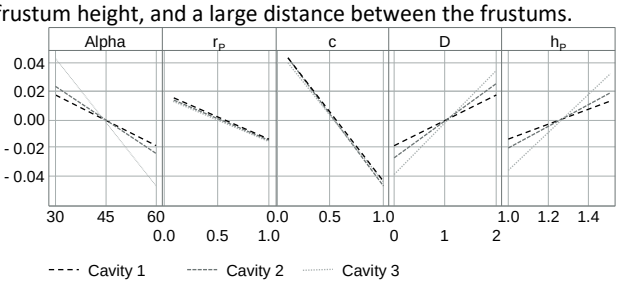

Figure 4. Main effects plots highlight the amount and direction of the influence of each main effect

Further analyses indicate that the difference in form filling between cavity (1) and (3) is particularly influenced by the pyramid angle. This difference decreases with flatter angles, larger frustum spacing (D), and greater frustum heights (h_P).

Minimizing the variation in form filling among cavities is, therefore, desirable for achieving uniform molding results. Consequently, optimizing process parameters such as molding temperature, pressing time, and pressing force can enhance global form accuracy and thereby improve overall cavity filling consistency.

3.2. Stress and flow behavior under the influence of inter-cavity geometry

Another significant consideration is the impact of the open tool concept without any flow barrier to limit the material flow out of the tool, which serves as a major disturbance for the outer cavity, as illustrated in Figure 5. The outward-directed glass flow differs substantially from the inner regions, indicating the variation in significant factors between the cavities (1) and (3).

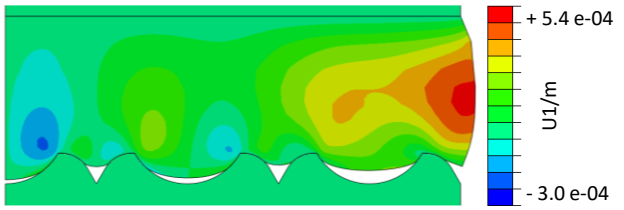

Figure 5. Displacement of glass in X-direction illustrating cavity-specific filling behavior and edge disturbance.

The pronounced influence of the pyramid angle on the filling behavior of the outer cavity can be attributed to the flow resistance encountered in the X-direction. It is observed that a flatter angle reduces flow resistance, whereas steeper angles generate larger lateral forces that impede material flow. This phenomenon is also observed in the other cavities at large angles and narrow frustum spacings (D), leading to self-locking (Figure 5) that impedes the glass flow between the gaps. The resulting increased flow resistance affects the filling of all cavities. It is evident that mold geometries exhibiting well-filled cavities also facilitate improved filling in inter-cavity regions.

The analyses of hydrostatic pressure (Figure 6) further confirm their critical role in determining cavity filling. Initial contact during the pressing occurs along the bridge width (c). The numerical analyses show that smaller bridge widths generate contact stresses nearly an order of magnitude higher than those for larger widths, as stress magnitude scales inversely with contact area.

This externally applied stress induces viscous deformation and initiates glass flow, while the resulting internal stresses relax over time (τ_R) due to the viscoelastic nature of glass at high temperature forming, described as below (eq. 5, 6):

$$\sigma(t) = \sigma_0 e^{-\frac{G(t-t_0)}{\eta}} = \sigma_0 e^{-\frac{(t-t_0)}{\tau_R}} \quad (5)$$

$$\tau_R = \frac{\eta}{G} \quad (6)$$

Moreover, the temporal evolution of hydrostatic pressure (Figure 6) highlights the influence of additional geometric factors. During continuous pressing, the glass initially contacts the radius and subsequently the flank defined by the pyramid angle. This sequence is evident in the characteristic stress decay patterns, which vary with both radius and angle.

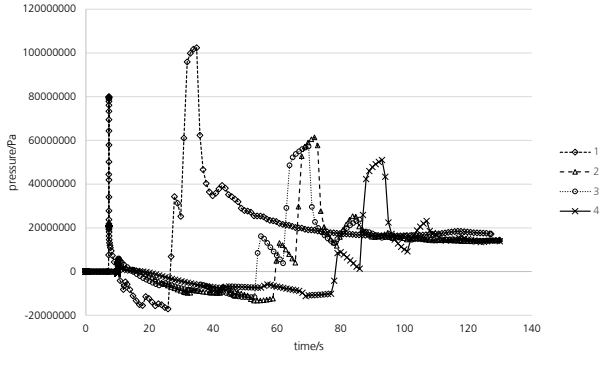

Figure 6. Hydrostatic pressure in cavity 1 for different mold geometries displayed over pressing time.

The temporal progression of hydrostatic pressure in cavity (1) (Figure 6) provides insights into the influence of different tool geometries (Figure 7), specifically:

- Geometry 1 (small r_P, small c, a flat a, large D, and high h_P): hydrostatic stress reaches ~90 MPa after 35 s, followed by relaxation; the form filling achieves 99.4 %.
- Geometry 2, identical except for a larger bridge width (c), exhibits a stress peak of ~61 MPa at 60 s, resulting in 92.1% form filling.
- Geometry 3 (larger r_P, steeper a, small c and D, low h_P) reaches ~58 MPa at 60 s with 86.8% filling.
- Geometry 4, similar to geometry 3 but with a larger (c), gets a peak at ~51 MPa at 90 s, and 79.3% form filling.

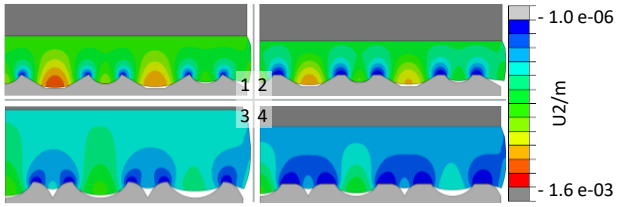

Figure 7. Comparison of the form filling for different mold geometries

In conclusion, it can be observed that a small initial contact area, defined as the sum of the bridge width (c) and the radius (r_P), is advantageous for the forming process. Smaller contact areas, in fact, generate higher initial shear stresses, which facilitate glass flow initiation. Additionally, the distance between adjacent frustum edges, expressed as $D+2b_P$ (Figure 8), plays a key role in determining penetration and flow uniformity, given that h_P is sufficiently high. Larger distances enable the tool to penetrate the glass more effectively, promoting improved cavity filling and overall molding efficiency. In particular, the surface ratio φ (eq. 7) should be maximized.

$$\varphi = \frac{D + 2b_P}{D + 2(b_P + \mathrm{C} + \mathrm{r}_P)} \tag{7}$$

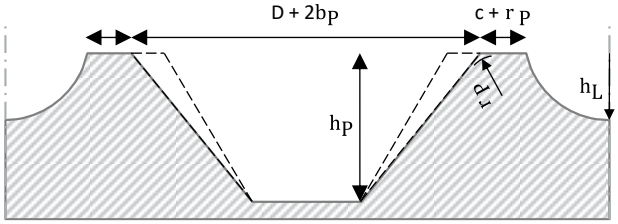

Figure 8. Design recommendations for the inter-cavity mold geometry for improved glass flow and form filling

The geometry of the mold, the individual cavities, and the inter-cavity regions induce the shear stresses (τ_S), which promote the material flow into both the cavities and the interstitial gaps. A reduced initial contact area effectively converts the applied load into high local contact stresses, which initiate shear within the glass and induce shape deformation. Shear stresses are directly influenced by contact friction and applied pressure. Furthermore, the shear strain rate ($\dot{\gamma}$) is directly linked to temperature-dependent viscosity and shear stress (eq. 8), such that higher shear stresses result in increased shear strain rates, thereby enhancing glass deformation.

$$\dot{\gamma} = \frac{\tau_S}{\eta(T)} \tag{8}$$

Resistance against shear-induced shape changes is generally lower than normal stress-induced changes in volume. This behavior is particularly pronounced for low compressibility materials like glass. Using this relation, the influence of the distance between the frustum edges can be elucidated: the greater this distance, the more glass is available between the areas to be formed. Consequently, the contribution of volumetric change per unit volume is lower than that observed with a smaller distance, leading to higher deviatoric stresses and, hence, increased form filling.

4. Conclusion

This numerical study demonstrates that inter-cavity geometry decisively governs form filling in WLGM. Using FE simulations of a 5×5 lens array with Schott B270® glass, combined with a DoE approach and RSM method, we are able to quantify how key geometric parameters, including bridge width (c), frustum radius (r_P), frustum height (h_P), pyramid angle (α), and frustum spacing (D), influence glass flow and the resulting stress state during pressing. Form filling was assessed relative to target cavity heights, and robust statistical analyses (ANOVA) showed strong and consistent trends across cavities, with the intermediate cavity most closely following its neighbors.

The main findings are here summarized: (i) a small initial contact area, realized by small c and small r_P, concentrates local stresses and initiates shear-driven flow into the cavities, improving fill; (ii) shear stresses dictate the filling behavior of the cavity due to glass's low compressibility, making shear-induced deformation preferable over normal stress-induced deformation; (iii) pyramid angle and frustum spacing modulate flow resistance, with flatter angles and larger spacing reducing hindrance and promoting more uniform filling across the array; (iv) edge effects arising from open tool concept can be mitigated by parameter choices that reduce center-to-edge fill disparities.

These insights translate into practical guidelines for the design of molding tools in WLGM, allowing the reduction of cycle times and improvement of material utilization while achieving high geometric accuracy across lens arrays. Future work should pursue experimental validation and further generalization of the recommendations to other process environments and geometries.

References

[1] Vu A T 2023 Modeling relaxation nature of nonequilibrium glass in nonisothermal glass molding

[2] Strobl C, Vogel P A, Vu A T, Mende H, Grunwald T, Schmitt R H and Bergs T 2022 Enabling Sustainability in Glass Optics Manufacturing by Wafer Scale Molding, The **25**th International Conference on Material Forming **926** 2371–2381

[3] Vogel P A, Strobl C and Mende H 2020 Verbundvorhaben: EFFEkT - Energie- und ressourceneffiziente Prozesskette zur Fertigung komplexer Glasoptiken: Teilvorhaben: Entwicklung eines Blankpressprozesses: Abschlussbericht: Berichtszeitraum: 01.12.2015-30.11.2019, Fraunhofer-Institut für Produktionstechnologien (IPT)

[4] Hünten M, Hollstegge D, Wang F, Dambon O and Klocke F 2011 Wafer level glass optics: precision glass molding as an alternative manufacturing approach, in: *Advanced Fabrication Technologies for Micro/Nano Optics and Photonics IV*, San Fancisco, California, United States, SPIE, pp. 94–100

[5] Liu G, Staasmeyer J H, Grunwald T, and Dambon O 2018 Scalability of the precision glass molding process for an efficient optics production, in: Optical Manufacturing and Testing XII, *SPIE*, Bellingham, Washington, USA, pp. 95–103

[6] Vu A T, Vogel P A, Dambon O and Klocke F 2018 Vacuum-assisted precision molding of 3D thin microstructure glass optics, in: *Fiber Lasers and Glass Photonics: Materials through Applications*, Strasbourg, France, SPIE, Bellingham, Washington, USA, p. 11.

[7] Hünten M 2014 Modellbildung für das Warmumformen von Glas, Apprimus

[8] Bernhardt F 2016 Entwicklung eines Verschleißmodells auf Basis der Degradationsmechanismen von Platin-Iridium-Beschichtungen beim Glaspressen, first. Aufl., Apprimus Wissenschaftsverlag, s.l.

[9] Vu A T, Grunwald T and Bergs T 2024 Friction in glass forming: Tribological behaviors of optical glasses and uncoated steel near glass transition temperature, *Journal of non-crystalline solids* **642**, 123160